Original Article | Thoracic Imaging

https://doi.org/10.3348/kjr.2018.19.6.1187
pISSN 1229-6929 · eISSN 2005-8330
Korean J Radiol 2018;19(6):1187-1195

Korean Journal of Radiology
KJR

Impact of Model-Based Iterative Reconstruction on the Correlation between Computed Tomography Quantification of a Low Lung Attenuation Area and Airway Measurements and Pulmonary Function Test Results in Normal Subjects

Da Jung Kim, MD[1]*, Cherry Kim, MD, PhD[1]*, Chol Shin, MD, PhD[2], Seung Ku Lee, PhD[3], Chang Sub Ko, BS[1], Ki Yeol Lee, MD, PhD[1]

Departments of [1]Radiology, [2]Pulmonology, and [3]Institute for Human Genomic Study, Korea University College of Medicine, Korea University Ansan Hospital, Ansan 15355, Korea

Objective: To compare correlations between pulmonary function test (PFT) results and different reconstruction algorithms and to suggest the optimal reconstruction protocol for computed tomography (CT) quantification of low lung attenuation areas and airways in healthy individuals.

Materials and Methods: A total of 259 subjects with normal PFT and chest CT results were included. CT scans were reconstructed using filtered back projection, hybrid-iterative reconstruction, and model–based IR (MIR). For quantitative analysis, the emphysema index (EI) and wall area percentage (WA%) were determined. Subgroup analysis according to smoking history was also performed.

Results: The EIs of all the reconstruction algorithms correlated significantly with the forced expiratory volume in one second (FEV1)/forced vital capacity (FVC) (all $p < 0.001$). The EI of MIR showed the strongest correlation with FEV1/FVC ($r = -0.437$). WA% showed a significant correlation with FEV1 in all the reconstruction algorithms (all $p < 0.05$) correlated significantly with FEV1/FVC for MIR only ($p < 0.001$). The WA% of MIR showed the strongest correlations with FEV1 ($r = -0.205$) and FEV1/FVC ($r = -0.250$). In subgroup analysis, the EI of MIR had the strongest correlation with PFT in both ever-smoker and never-smoker subgroups, although there was no significant difference in the EI between the reconstruction algorithms. WA% of MIR showed a significantly thinner airway thickness than the other algorithms (49.7 ± 7.6 in ever-smokers and 49.5 ± 7.5 in never-smokers, all $p < 0.001$), and also showed the strongest correlation with PFT in both ever-smoker and never-smoker subgroups.

Conclusion: CT quantification of low lung attenuation areas and airways by means of MIR showed the strongest correlation with PFT results among the algorithms used, in normal subjects.

Keywords: *Computed tomography; Iterative reconstruction; Pulmonary emphysema; Airway; Pulmonary function test*

Received March 20, 2018; accepted after revision June 28, 2018.
This study was supported by a National Research Foundation of Korea (NRF) grant funded by the Korean government (MSIP) (NRF-2016R1A2B4012155), and Korea Centers for Disease Control and Prevention (2015-P71001-00).
This study was supported by Reyon Pharmaceutical (I1704621) and Philips Company (I0902491).
*These authors contributed equally to this work.
Corresponding author: Ki Yeol Lee, MD, PhD, Department of Radiology, Korea University College of Medicine, Korea University Ansan Hospital, 123 Jeokgeum-ro, Danwon-gu, Ansan 15355, Korea.
• Tel: (8231) 412-5227 • Fax: (8231) 412-4264 • E-mail: kiylee@korea.ac.kr

INTRODUCTION

Computed tomography (CT) is increasingly being used in clinical applications (1). In particular, CT-based quantification of pulmonary function by means of CT densitometry has been shown to yield reproducible results, when using the same acquisition protocol (2-5). In patients with chronic obstructive pulmonary disease (COPD), CT-based quantification of emphysema volume and airway thickness has also been validated as a method that yields results that match relatively well with those of pulmonary function tests (PFTs) (6, 7). Furthermore, CT quantification results of the lungs and airways showed significant correlations with PFT results in subjects with normal spirometry; CT quantification parameters may also differ significantly according to smoking history (8). Therefore, the use of CT for quantification of pulmonary function in patients with COPD as well as in healthy individuals is expected to increase in future.

However, the increase in radiation exposure of the population due to this increased CT usage has garnered attention. Much effort has focused on reducing the radiation dose while still maintaining sufficient image quality. Specifically, iterative reconstruction (IR) techniques are being used for some applications. These techniques can potentially decrease radiation exposure and are able to replace the conventional filtered back projection (FBP) (9-15). However, the measured CT densitometry results are affected by different image reconstruction approaches, even when the initial CT image data sets are derived from a single individual (16). Although several studies have examined the effects of different IR algorithms, including hybrid-IR (HIR) and model-based IR (MIR), on emphysema quantification (17-19), to our knowledge, correlations between PFT results and these IR algorithms have not been investigated in healthy individuals to date.

Therefore, the aims of this study were to compare correlations between PFT results and different reconstruction algorithms and to suggest an optimized reconstruction protocol for CT quantification of the low lung attenuation area and airways in healthy individuals.

MATERIALS AND METHODS

This retrospective study was approved by our Institutional Review Board and the requirement for obtaining informed consent was waived.

Clinical Subjects

The study group consisted of 259 participants in the Ansan cohort included in the Korean Genome Epidemiology Study; these individuals had normal PFT and chest CT scan results. PFT was performed in each subject within 1 week prior to referral for CT scanning. The exclusion criteria were: 1) underlying lung disease, including asthma or pulmonary tuberculosis, 2) taking anti-inflammatory medication, 3) previous surgical lung resection, and 4) severe motion artifacts in the chest CT scan. Finally, 223 subjects were selected for the analysis (120 males and 103 females). Among these subjects, 141 were never-smokers, 63 were ex-smokers, and 19 were smokers. We defined ex-smokers and current smokers as ever-smokers. Clinical data, including smoking history (never-smokers and ever-smokers), height, weight, and body mass index (BMI), were also recorded.

CT Acquisition and Image Reconstruction

All CT images were acquired with a 64-channel multi-detector CT scanner (Brilliance 64; Philips Healthcare, Cleveland, OH, USA). The following CT scanning parameters were employed: detector configuration, 64 x 0.625 mm; rotation time, 0.5 seconds; tube voltage, 120 kVp; tube current, 75 mAs without current modulation; section thickness, 0.625 mm. Contrast injection was not performed. Each subject was examined in the supine position with a breath hold on a deep inspiratory breath.

Raw data were reconstructed using three different reconstruction algorithms: FBP, HIR (iDose^4; Philips Healthcare), and MIR (IMR; Philips Healthcare). For MIR, three different image definitions were used (IMR-R1, MIR with "body routine"; IMR-ST1, MIR with "soft tissue"; and IMR-SP1, MIR with "sharp plus"; Philips Healthcare) (Fig. 1). For quantification of the low lung attenuation area volume, four reconstruction algorithms were applied (FBP, HIR, IMR-R1, and IMR-ST1). For airway quantification, three reconstruction algorithms were applied (FBP, HIR, and IMR-SP1). For noise reduction, level 4 was used for HIR and level 1 was used for MIR.

Image Analysis

The CT images were analyzed with an automated lung image analysis tool (IntelliSpace Portal 7.0; Philips Healthcare). This tool performs 4 steps: lung segmentation, lung density measurement, airway extraction, and airway measurement. The lungs and lobes are segmented using a model-based algorithm and the trachea are extracted

Korean Journal of Radiology
KJR

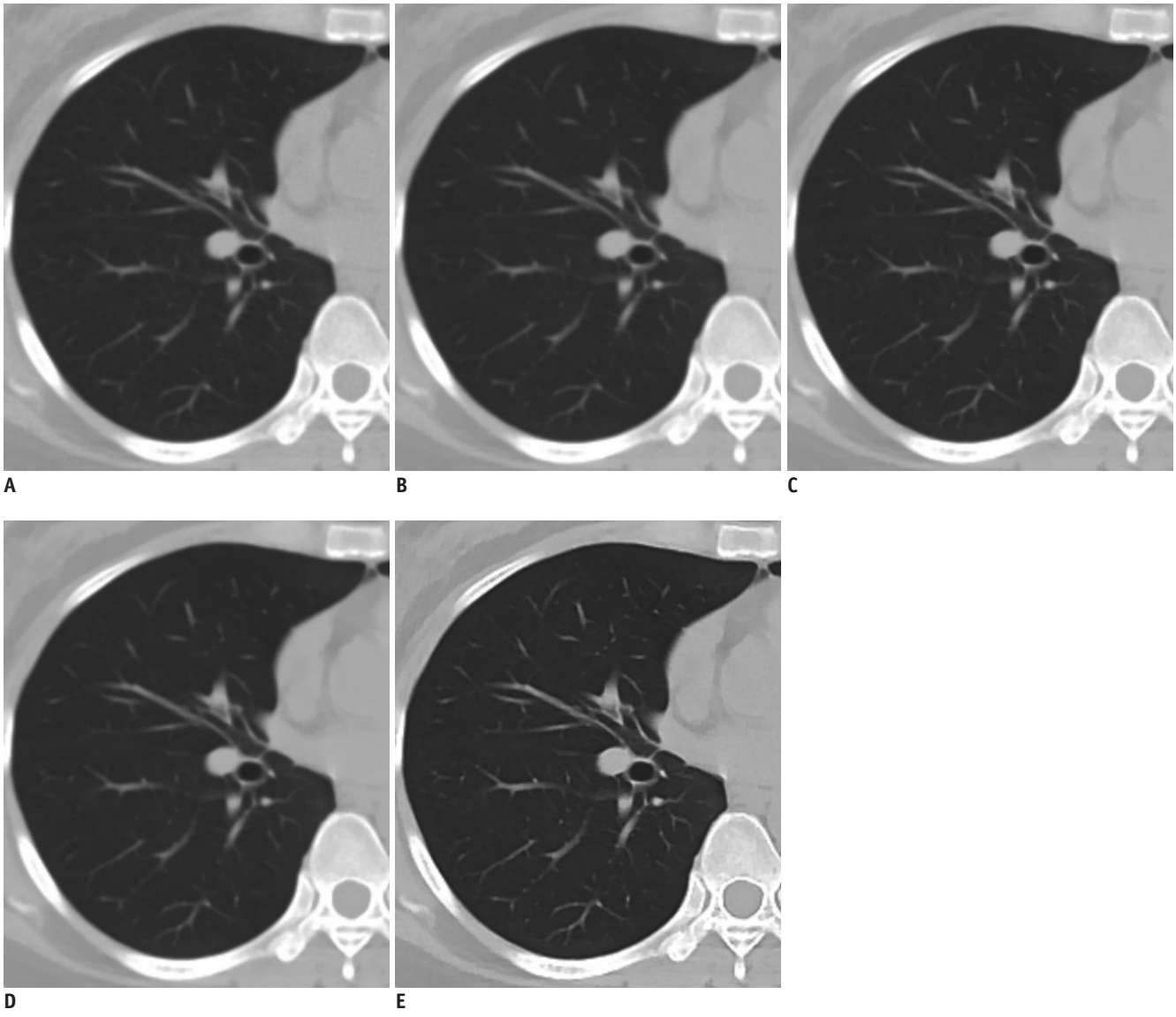

Fig. 1. Axial CT images of study population.
A. Filtered back projection. **B.** Hybrid iterative reconstruction (iDose^4; Philips Healthcare). **C.** MIR (IMR with "body routine" image definition [IMR-R1; Philips Healthcare]). **D.** MIR (IMR with "soft tissue" image definition [IMR-ST1; Philips Healthcare]). **E.** MIR (IMR with "sharp plus" image definition [IMR-SP1; Philips Healthcare]). CT = computed tomography, MIR = model-based iterative reconstruction

automatically to verify airway extraction. The low lung attenuation area threshold can be preselected; -950 HU was used in this study. For quantitative analysis of the low lung attenuation area volume, classical indexes of emphysema parameters, including total lung volume, emphysema volume with a threshold of -950 HU, and emphysema index (EI), were obtained automatically (Fig. 2A).

For quantitative analysis of airway wall thickness, the Weinheimer method was used. In brief, the proximal portion of the right upper lobe apical segmental bronchus was selected, after which several parameters were measured automatically at that bronchus: luminal area (LA), airway wall area (WA), and wall area percentage (WA% = WA / [WA + LA]) (Fig. 2B).

Pulmonary Function Test

Forced spirometry was performed before and after applying bronchodilator in all subjects. PFT parameters are expressed in liters and percentages. The following spirometric values were investigated for the extent of their correlation with CT parameters: forced expiratory volume in 1 second (FEV1), forced vital capacity (FVC), and the ratio of FEV1 to FVC after bronchodilation (FEV1/FVC).

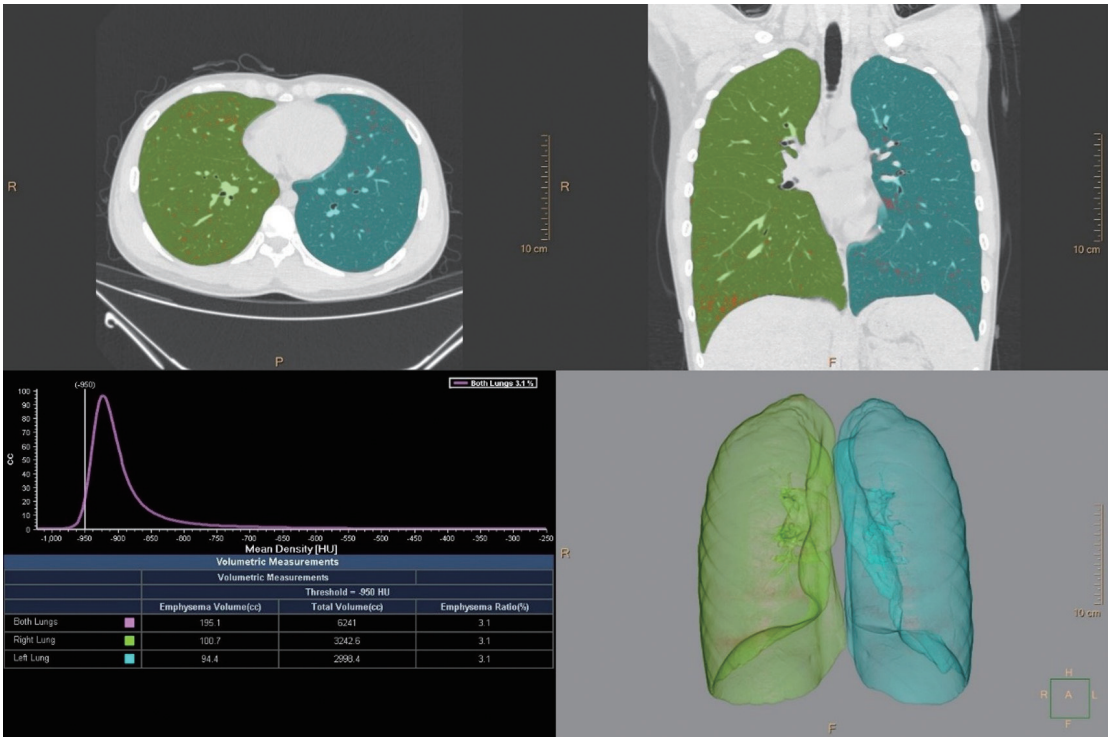

A

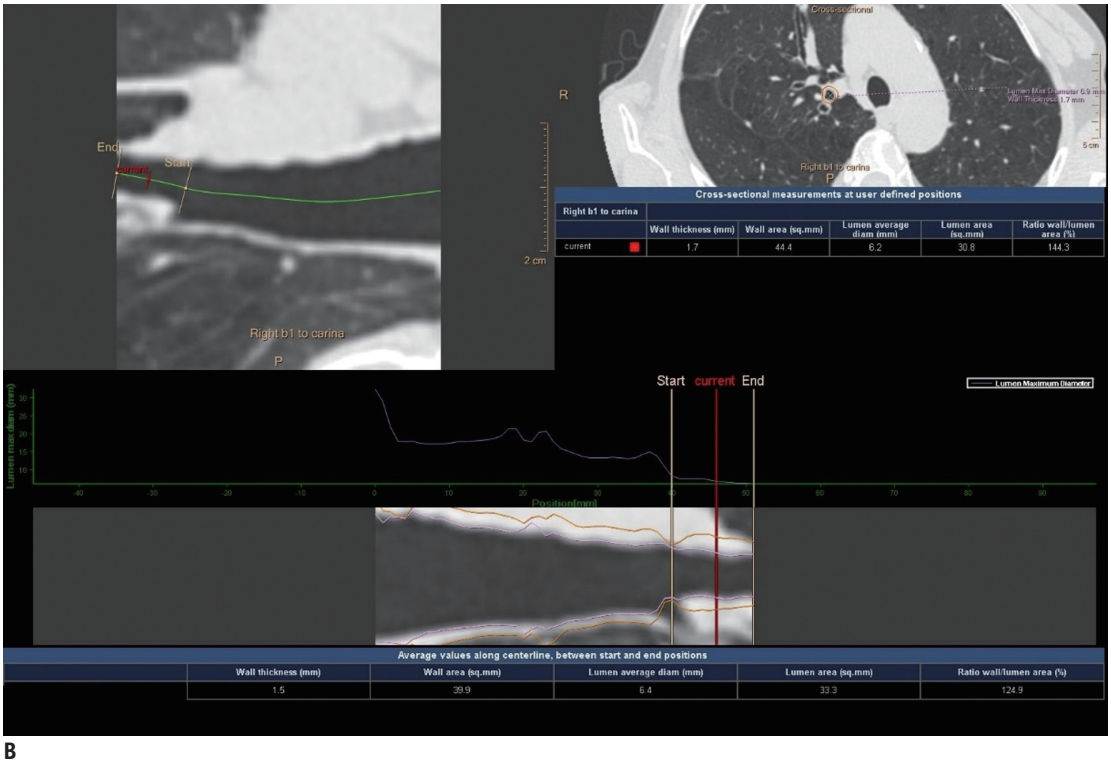

B

Fig. 2. Representative example of CT quantification of low lung attenuation area and airway from 64-year-old male.
A. For quantitative analysis of low lung attenuation area, -950 HU was used as threshold. Area under -950 HU curve is displayed as red-dotted area. **B.** For quantitative analysis of airway thickness, three-dimensional image of tracheobronchial tree was automatically generated. Then, segment of bronchus of right upper lobe, from most proximal portion to bifurcation, was selected. In this area, average value of each of several airway parameters, including LA, WA, and WA% (WA% = WA / [WA + LA]) were automatically measured. LA = luminal area, WA = wall area, WA% = wall area percentage

Korean Journal of Radiology
KJR

Statistical Analysis

Demographic variables are expressed as means ± standard deviations. Differences in the low lung attenuation area or airway measurements were compared between algorithms using one-way analysis of variance. Bonferroni's post-hoc test was performed for multiple comparisons. Subgroup analysis was performed according to smoking history; baseline characteristics were compared between never-smokers and ever-smokers using Student's *t* test for continuous variables and using the chi-square test for categorical variables.

Pearson's correlation coefficients were calculated and linear regression analysis was conducted to evaluate the extent of correlation between different algorithms and PFT results in the overall cohort and in subgroups defined by smoking history. Statistical analyses were performed using SAS version 9.3 (SAS Institute Inc., Cary, NC, USA) and the SPSS package, version 20.0 (IBM Corp., Armonk, NY, USA). All p values < 0.05 were considered statistically significant.

RESULTS

Baseline Characteristics

The baseline characteristics of the overall study subjects, never-smokers, and ever-smokers are shown in Table 1. The overall study subjects were divided into two subgroups: 141 never-smokers and 82 ever-smokers. Sex distribution was significantly different between the two subgroups (p < 0.001). Specifically, all the enrolled females were in the never-smokers group, while the ever-smokers consisted of only male subjects. There were significant differences in height and weight (all p < 0.001), although BMI did not show a significant difference between the two subgroups. PFT results, including FEV1, FVC, and FEV1/FVC, were significantly higher in never-smokers than in ever-smokers (all p < 0.05).

Low Lung Attenuation Area and Airway Measurements

Table 2 compares the mean EI and WA% values for each algorithm. EI was not significantly different between any of the algorithms (p = 0.83). However, WA% was significantly

Table 1. Baseline Characteristics of Study Cohort

Subject Characteristics	Total (n = 223)	Never-Smokers (n = 141)	Ever-Smokers (n = 82)	*P*
Age (years)	63.6 ± 6.6	63.6 ± 6.9	63.7 ± 6.2	0.916
Sex (%)				< 0.001
Male	120 (53.8)	38 (31.7)	82 (36.8)	
Female	103 (46.2)	103 (100)	0 (0)	
BMI (kg/m^2)	24.0 ± 2.9	23.9 ± 3.1	24.3 ± 2.3	0.313
Height (cm)	161.5 ± 8.0	158.2 ± 7.1	167.2 ± 5.8	< 0.001
Weight (kg)	62.9 ± 9.7	59.9 ± 9.2	68.0 ± 8.3	< 0.001
PFT				
FEV1 (% predicted)	108.7 ± 16.8	111.6 ± 17.3	103.5 ± 14.5	< 0.001
FVC (% predicted)	100.4 ± 13	101.7 ± 13.4	98.1 ± 11.9	0.028
FEV1/FVC (%)	77.3 ± 8.3	78.9 ± 8.3	74.6 ± 7.7	< 0.001

All data are expressed as means ± standard deviations. BMI = body mass index, FEV1 = forced expiratory volume in one second after bronchodilators, FVC = forced vital capacity after applying bronchodilators, FEV1/FVC = ratio of FEV1 to FVC after applying bronchodilators, PFT = pulmonary function test

Table 2. Mean EI and WA% Values in All Study Subjects*

EI				
FBP	HIR	IMR-R1	IMR-ST1	*P*
1.3 ± 3.5 (0.0–40.1)	1.0 ± 3.6 (0.0–38.2)	1.2 ± 3.6 (0.0–34.5)	1.1 ± 3.6 (0.0–34.6)	0.83
WA%				
FBP	HIR	IMR-SP1		*P*
55.5 ± 9.6 (36.6–113.3)	55.7 ± 9.1 (34.8–115.4)	49.6 ± 7.6 (25.2–97.3)		< 0.001

*IMR-R1, Philips Healthcare; IMR-ST1, Philips Healthcare; IMR-SP1, Philips Healthcare. EI = emphysema index, FBP = filtered back projection, HIR = hybrid-iterative reconstruction, IMR-R1 = MIR with "body routine" image definition, IMR-SP1 = MIR with "sharp plus" image definition, IMR-ST1 = MIR with "soft tissue" image definition, MIR = model-based iterative reconstruction, WA% = wall area percentage

lower in IMR-SP1 than in FBP and HIR ($p < 0.001$).

Correlation between CT Quantification Measurements and Pulmonary Function Test Results

The correlations between CT quantification measurements and PFT results for each reconstruction algorithm are shown in Table 3. In terms of correlations between EI and PFT results, FEV1/FVC showed a significant negative correlation with EI for all reconstruction algorithms (all $p < 0.001$), while EI of IMR-R1 showed the strongest correlation with FEV1/FVC ($r = -0.437$). In terms of correlations between WA% and PFT results, FEV1 showed a significant negative correlation with WA% for all the reconstruction algorithms (all $p < 0.05$), while WA% of IMR-SP1 showed the strongest correlation with FEV1 ($r = -0.205$). However, FEV1/FVC correlated significantly with WA% only in IMR-SP1 ($r = -0.250$). In linear regression analysis, the EIs of FBP, HIR, IMR-R1, and IMR-ST1, and WA% of IMR-SP1 were significant independent predictors of FEV1/FVC. WA% of FBP, HIR, and IMR-SP1 were also significant independent predictors of FEV1.

Subgroup Analysis according to Smoking History

Tables 4 and 5 show the results of the subgroup analysis according to smoking history (ever-smokers vs. never-smokers). EI did not show significant differences between any of the algorithms in either the ever-smoker or never-smoker subgroup ($p = 0.882$ and $p = 0.802$, respectively). However, WA% of IMR-SP1 was significantly lower than that of FBP and HIR in both the ever-smoker and never-smoker subgroups (all $p < 0.001$). EI was significantly higher in the ever-smoker than in the never-smoker subgroup for all reconstruction algorithms (all $p < 0.001$). While WA% was higher in the ever-smoker subgroup than in the never-smoker group in all reconstruction algorithms, the differences were not significant ($p = 0.062$ in FBP, $p = 0.232$ in HIR, and $p = 0.981$ in MIR).

In the ever-smoker subgroup, the EI of HIR and IMR-R1 showed a significant negative correlation with FEV1, and EIs in all the algorithms had significant negative correlations with FEV1/FVC. Among these algorithms, the EI of IMR-R1 showed the strongly correlation with FEV1 ($r = -0.246$) and FEV1/FVC ($r = -0.409$). In the never-smoker subgroup, all algorithms showed a significant negative correlation between EI and FEV1/FVC, and IMR-R1 also demonstrated the strongest correlation with FEV1/FVC ($r = -0.515$). In the linear regression analysis, EIs of all the reconstruction algorithms were significant independent predictors of FEV1/FVC in both subgroups. The highest R^2 value was observed for IMR-R1 among both ever-smokers and never-smokers

Table 3. Correlation Coefficient (r) and R^2 between Quantitative CT Measurements of Low Lung Attenuation Area and Airway and PFT Results in Each Reconstruction Algorithm in Overall Study Cohort

	EI				WA%		
	FBP	HIR	IMR-R1	IMR-ST1	FBP	HIR	IMR-SP1
FEV1							
r	-0.048	-0.088	-0.083	-0.083	-0.155*	-0.139*	-0.205**
Adjusted R^2					0.018	0.019	0.042
β					-0.009*	-0.009*	-0.015**
FEV1/FVC							
r	-0.397***	-0.400***	-0.437***	-0.410***	-0.118	-0.130	-0.250***
Adjusted R^2	0.157	0.160	0.191	0.168			0.062
β	-0.957***	-0.933***	-1.016***	-0.957***			-0.305***

*$p < 0.05$, **$p < 0.01$, ***$p < 0.001$. R^2 = adjusted R-square values

Table 4. Mean EI and WA% Values according to Smoking History

	FBP	HIR	IMR-R1	IMR-ST1	*P*
EI					
Ever-smokers	2.2 ± 5.2 (0.03–40.1)	1.7 ± 5.3 (0.01–38.2)	1.8 ± 5.0 (0.05–34.5)	1.6 ± 5.0 (0.0–34.6)	0.882
Never-smokers	0.76 ± 1.5 (0.1–14.4)	0.63 ± 1.8 (0.0–18.6)	0.87 ± 2.3 (0.02–22.5)	0.75 ± 2.3 (0.0–22.5)	0.802
	FBP	HIR	IMR-SP1		*P*
WA%					
Ever-smokers	57.6 ± 10.7 (42.2–113.3)	57.0 ± 10.6 (34.8–115.4)	49.7 ± 7.6 (31.6–97.3)		< 0.001
Never-smokers	54.4 ± 8.8 (26.6–77.0)	55.0 ± 8.1 (36.8–74.8)	49.5 ± 7.5 (25.2–77.8)		< 0.001

Korean Journal of Radiology
KJR

Table 5. Correlation Coefficient (*r*) and R^2 between Quantitative CT Measurements of Low Lung Attenuation Area and Airway and PFT Results in Each Reconstruction Algorithm according to Smoking History

	EI				WA%		
	FBP	HIR	IMR-R1	IMR-ST1	FBP	HIR	IMR-SP1
Ever-Smokers							
FEV1							
r	-0.172	-0.229*	-0.246*	-0.157	-0.29**	-0.231*	-0.237*
Adjusted R^2		0.053	0.06		0.084	0.053	0.056
β		-0.085*	-0.083*		-0.002**	-0.002*	-0.004*
FEV1/FVC							
r	-0.263*	-0.336**	-0.409***	-0.234*	-0.181	-0.123	-0.211
Adjusted R^2	0.069	0.113	0.167	0.055			
β	-1.222*	-2.269**	-2.517***	-1.216*			
Never-Smokers							
FEV1							
r	-0.053	-0.070	-0.055	-0.060	-0.132	-0.175	-0.32***
Adjusted R^2							0.045
β							0.013*
FEV1/FVC							
r	-0.457***	-0.514***	-0.515***	-0.507***	-0.043	-0.123	-0.436***
Adjusted R^2	0.209	0.229	0.264	0.257			0.190
β	-0.914***	-0.903***	-0.972***	-0.970***			-0.436***

*p < 0.05, **p < 0.01, ***p < 0.001.

(ever-smokers, R^2 = 0.167; never-smokers, R^2 = 0.264). The EIs in HIR and IMR-R1 were significant independent predictors of FEV1, but only in the ever-smoker subgroup.

In terms of the correlations between WA% and PFT results, FEV1 showed significant negative correlations for all reconstruction algorithms in the ever-smoker subgroup, whereas WA% of only IMR-SP1 showed a significant negative correlation with FEV1 in the never-smoker subgroup. However, in terms of the correlations between WA% and FEV1/FVC, only IMR-SP1 in the never-smoker subgroup demonstrated a significant negative correlation (r = -0.436). In linear regression analysis, WA% of all the reconstruction algorithms in the ever-smoker subgroup was a significant independent predictor of FEV1. In the never-smoker subgroup, however, WA% of IMR-SP1 was the only significant independent predictor of FEV1 and FEV1/FVC.

DISCUSSION

This study demonstrated a correlation between PFT results and CT quantification using different reconstruction algorithms in normal study subjects. Overall, the EIs of all the reconstruction algorithms, involving FBP, HIR, and MIR (IMR-R1 and IMR-ST1) showed significant correlations with FEV1/FVC. Among these, the EI of MIR (IMR-R1) had the strongest correlation with FEV1/FVC. Among the algorithms, WA% of MIR (IMR-SP1) demonstrated a significant correlation and the strongest correlation with FEV1 and FEV1/FVC, respectively. In the subgroup analysis, the EI measured by MIR (IMR-R1) had the strongest correlation with PFT in both the ever-smoker and the never-smoker subgroups, although the EI did not differ significantly between the reconstruction algorithms. Among the different algorithms, only MIR (IMR-SP1) also yielded a significantly thinner airway thickness than the other algorithms. Moreover, airway measurement in MIR showed the strongest correlation with PFT in both the ever-smoker and never-smoker subgroups.

Several studies have examined the effect of MIR on emphysema quantification in CT. In a recent prospective study, the EI was shown to decrease significantly with the use of MIR (20). Another study compared FBP and MIR (ADIR 3D; Canon Medical Systems, Tochigi, Japan), using different dose settings (21). In this study, the extent of emphysema was more consistent across different dose settings when using MIR than when using FBP. Nishio et al. (22) suggested that the use of MIR (ADIR 3D) could improve the consistency of emphysema quantification between low-dose and standard-dose CT. In our study, we demonstrated that the EI measured using MIR (IMR-R1) had the strongest

correlation with PFT, although there was no significant difference in the EI between the reconstruction algorithms. This finding could be explained by the lower mean EI of our study population than that reported in previous studies (1.3 ± 3.5 [EI of FBP in our study] versus 3.13 ± 0.59 [EI of FBP reported by Martin et al.]) (20). Moreover, our cohort included individuals with normal PFT results. In addition, the EI of our study population was similar to that of a previous study that reported on CT quantification of the lung and airways in normal Korean subjects (8).

Choo et al. (17) reported that airway wall measurements differed significantly among the three algorithms used, with MIR yielding thinner walls than adaptive statistical IR (ASIR) and FBP. Furthermore, MIR seemed to provide the most accurate measurements among all the algorithms (17); those authors also used a phantom to validate the accuracy of airway measurement using each reconstruction algorithm. The absolute measurement errors were lowest for MIR, in the increasing order of MIR, ASIR, and FBP. We also found that MIR (IMR-SP1) yielded significantly thinner airway thickness than did the other algorithms. In addition, airway measurement in MIR showed the strongest correlation with PFT. Based on these results, we inferred that the choice of reconstruction algorithm can affect the relationship between CT quantification measurement and PFT in the normal population. In addition, a suitable reconstruction algorithm must be selected to obtain the CT quantification measurement most relevant to PFT results.

In the analysis of subgroups defined by smoking history, we also demonstrated a correlation between CT measurement and PFT results for the different algorithms. In our study, the EI of MIR (IMR-R1) showed the strongest correlation with FEV1/FVC in both ever- and never-smokers. Moreover, WA% of MIR (IMR-SP1) showed a significant correlation with FEV1 in ever-smokers, and with both FEV1 and FEV1/FVC in never-smokers. Another recent study of normal subjects reported similar results: the bronchial wall thickness of the inner perimeter of the 10-mm diameter airway (Pi10) in ever-smokers correlated significantly with FEV1/FVC (8). Thus, we propose that MIR is the best reconstruction algorithm for CT quantification of the low lung attenuation area and airway, because the measurements in MIR showed the strongest correlation with the PFT results in both ever-smokers and never-smokers.

In previous studies, it was reported that MIR reduced image noise and artifacts and improved the visualization of thoracic structures in chest CT (23). Additionally, the non-linear image noise reduction by IMR improved both quantitative and qualitative image quality, allowing a further radiation dose reduction (23-26). The results from these previous studies seem to support our results that MIR is the best reconstruction algorithm for CT quantification of low lung attenuation area and airway, showing the best correlation with the PFT in the normal population with/without smoking history, although we did not analyze image quality of each reconstruction algorithm.

Our study had several limitations. First, the ever-smoker subgroup consisted entirely of males. Since there was a significant sex difference in the PFT results and CT measurements, this may have produced errors when evaluating the influence of smoking in a large cohort. Second, there was no standard reference for low lung attenuation area and airway quantification.

In conclusion, CT quantification of low lung attenuation area and airway using MIR showed a better correlation with PFT results than did HIR and FBP, in normal subjects. These results indicate that CT using MIR is useful. They also provide more accurate values for quantitative measures of the low lung attenuation area and airway, as well as for morphologic assessment, in routine check-up of the normal population.

REFERENCES

1. Brenner DJ, Hall EJ. Computed tomography--an increasing source of radiation exposure. *N Engl J Med* 2007;357:2277-2284
2. Hackx M, Bankier AA, Gevenois PA. Chronic obstructive pulmonary disease: CT quantification of airways disease. *Radiology* 2012;265:34-48
3. Ceresa M, Bastarrika G, de Torres JP, Montuenga LM, Zulueta JJ, Ortiz-de-Solorzano C, et al. Robust, standardized quantification of pulmonary emphysema in low dose CT exams. *Acad Radiol* 2011;18:1382-1390
4. Newell JD Jr, Hogg JC, Snider GL. Report of a workshop: quantitative computed tomography scanning in longitudinal studies of emphysema. *Eur Respir J* 2004;23:769-775
5. Xie X, de Jong PA, Oudkerk M, Wang Y, Ten Hacken NH, Miao J, et al. Morphological measurements in computed tomography correlate with airflow obstruction in chronic obstructive pulmonary disease: systematic review and meta-analysis. *Eur Radiol* 2012;22:2085-2093
6. Chen H, Chen RC, Guan YB, Li W, Liu Q, Zeng QS. Correlation of pulmonary function indexes determined by low-dose MDCT with spirometric pulmonary function tests in patients with chronic obstructive pulmonary disease. *AJR Am J Roentgenol* 2014;202:711-718

7. Park KJ, Bergin CJ, Clausen JL. Quantitation of emphysema with three-dimensional CT densitometry: comparison with two-dimensional analysis, visual emphysema scores, and pulmonary function test results. *Radiology* 1999;211:541-547
8. Kim SS, Jin GY, Li YZ, Lee JE, Shin HS. CT quantification of lungs and airways in normal Korean subjects. *Korean J Radiol* 2017;18:739-748
9. Hara AK, Paden RG, Silva AC, Kujak JL, Lawder HJ, Pavlicek W. Iterative reconstruction technique for reducing body radiation dose at CT: feasibility study. *AJR Am J Roentgenol* 2009;193:764-771
10. Mayo-Smith WW, Hara AK, Mahesh M, Sahani DV, Pavlicek W. How I do it: managing radiation dose in CT. *Radiology* 2014;273:657-672
11. Geyer LL, Schoepf UJ, Meinel FG, Nance JW Jr, Bastarrika G, Leipsic JA, et al. State of the art: iterative CT reconstruction techniques. *Radiology* 2015;276:339-357
12. Kuo Y, Lin YY, Lee RC, Lin CJ, Chiou YY, Guo WY. Comparison of image quality from filtered back projection, statistical iterative reconstruction, and model-based iterative reconstruction algorithms in abdominal computed tomography. *Medicine (Baltimore)* 2016;95:e4456
13. Singh S, Kalra MK, Do S, Thibault JB, Pien H, O'Connor OJ, et al. Comparison of hybrid and pure iterative reconstruction techniques with conventional filtered back projection: dose reduction potential in the abdomen. *J Comput Assist Tomogr* 2012;36:347-353
14. Szilveszter B, Elzomor H, Károlyi M, Kolossváry M, Raaijmakers R, Benke K, et al. The effect of iterative model reconstruction on coronary artery calcium quantification. *Int J Cardiovasc Imaging* 2016;32:153-160
15. Padole A, Ali Khawaja RD, Kalra MK, Singh S. CT radiation dose and iterative reconstruction techniques. *AJR Am J Roentgenol* 2015;204:W384-W392
16. Boedeker KL, McNitt-Gray MF, Rogers SR, Truong DA, Brown MS, Gjertson DW, et al. Emphysema: effect of reconstruction algorithm on CT imaging measures. *Radiology* 2004;232:295-301
17. Choo JY, Goo JM, Lee CH, Park CM, Park SJ, Shim MS. Quantitative analysis of emphysema and airway measurements according to iterative reconstruction algorithms: comparison of filtered back projection, adaptive statistical iterative reconstruction and model-based iterative reconstruction. *Eur Radiol* 2014;24:799-806
18. Nishio M, Koyama H, Ohno Y, Negi N, Seki S, Yoshikawa T, et al. Emphysema quantification using ultralow-dose CT with iterative reconstruction and filtered back projection. *AJR Am J Roentgenol* 2016;206:1184-1192
19. Nishio M, Matsumoto S, Ohno Y, Sugihara N, Inokawa H, Yoshikawa T, et al. Emphysema quantification by low-dose CT: potential impact of adaptive iterative dose reduction using 3D processing. *AJR Am J Roentgenol* 2012;199:595-601
20. Martin SP, Gariani J, Hachulla AL, Botsikas D, Adler D, Karenovics W, et al. Impact of iterative reconstructions on objective and subjective emphysema assessment with computed tomography: a prospective study. *Eur Radiol* 2017;27:2950-2956
21. Yamashiro T, Miyara T, Honda O, Tomiyama N, Ohno Y, Noma S, et al. Iterative reconstruction for quantitative computed tomography analysis of emphysema: consistent results using different tube currents. *Int J Chron Obstruct Pulmon Dis* 2015;10:321-327
22. Nishio M, Matsumoto S, Seki S, Koyama H, Ohno Y, Fujisawa Y, et al. Emphysema quantification on low-dose CT using percentage of low-attenuation volume and size distribution of low-attenuation lung regions: effects of adaptive iterative dose reduction using 3D processing. *Eur J Radiol* 2014;83:2268-2276
23. Yuki H, Oda S, Utsunomiya D, Funama Y, Kidoh M, Namimoto T, et al. Clinical impact of model-based type iterative reconstruction with fast reconstruction time on image quality of low-dose screening chest CT. *Acta Radiol* 2016;57:295-302
24. Neroladaki A, Botsikas D, Boudabbous S, Becker CD, Montet X. Computed tomography of the chest with model-based iterative reconstruction using a radiation exposure similar to chest X-ray examination: preliminary observations. *Eur Radiol* 2013;23:360-366
25. Laqmani A, Avanesov M, Butscheidt S, Kurfürst M, Sehner S, Schmidt-Holtz J, et al. Comparison of image quality and visibility of normal and abnormal findings at submillisievert chest CT using filtered back projection, iterative model reconstruction (IMR) and iDose^{4TM}. *Eur J Radiol* 2016;85:1971-1979
26. Katsura M, Matsuda I, Akahane M, Yasaka K, Hanaoka S, Akai H, et al. Model-based iterative reconstruction technique for ultralow-dose chest CT: comparison of pulmonary nodule detectability with the adaptive statistical iterative reconstruction technique. *Invest Radiol* 2013;48:206-212